

See discussions, stats, and author profiles for this publication at: <https://www.researchgate.net/publication/275244181>

Diffusion of Benzene in the Breathing Metal–Organic Framework MIL–53(Cr): A Joint Experimental–Computational Investigation

ARTICLE *in* THE JOURNAL OF PHYSICAL CHEMISTRY C · APRIL 2015

Impact Factor: 4.77 · DOI: 10.1021/acs.jpcc.5b01465

CITATIONS

2

READS

108

8 AUTHORS, INCLUDING:



Pascal G. Yot

Université de Montpellier

54 PUBLICATIONS 683 CITATIONS

SEE PROFILE



Jacques Ollivier

Institut Laue-Langevin

122 PUBLICATIONS 1,015 CITATIONS

SEE PROFILE



Philippe Trens

Ecole Nationale Supérieure de Chimie de Mo...

82 PUBLICATIONS 1,197 CITATIONS

SEE PROFILE



Alexander G Stepanov

Boreskov Institute of Catalysis

136 PUBLICATIONS 1,677 CITATIONS

SEE PROFILE

Diffusion of Benzene in the Breathing Metal–Organic Framework MIL-53(Cr): A Joint Experimental–Computational Investigation

D. I. Kolokolov,^{†,‡} H. Jobic,^{*,‡} S. Rives,^{‡,§} P. G. Yot,[§] J. Ollivier,^{||} P. Trens,[⊥] A. G. Stepanov,^{†,‡} and G. Maurin^{*,§}

[†]Boreskov Institute of Catalysis, Siberian Branch of Russian Academy of Sciences, Prospekt Akademika Lavrentieva 5, Novosibirsk 630090, Russia

[‡]Institut de Recherches sur la Catalyse et l'Environnement de Lyon, CNRS, Université de Lyon, 2. Av. A. Einstein, 69626 Villeurbanne, France

[§]Institut Charles Gerhardt Montpellier, UMR 5253 UM CNRS ENSCM, Université Montpellier, Place E. Bataillon, Montpellier cedex 05, 34095, France

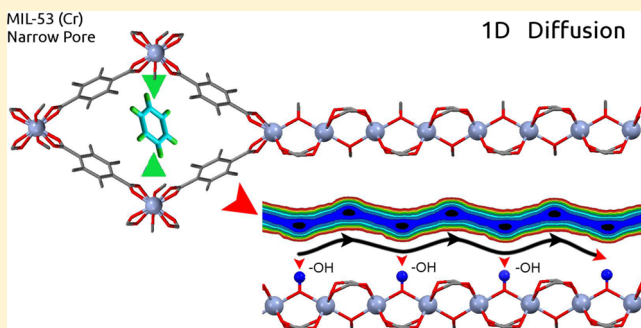
^{||}Institut Laue Langevin, BP 156, 38042 Grenoble, France

[⊥]Institut Charles Gerhardt Montpellier, UMR 5253 CNRS UM ENSCM UM1, Ecole Nationale Supérieure de Chimie Montpellier, 8 rue de l'Ecole Normale, cedex 05, 34296, France

^{*}Novosibirsk State University, Faculty of Natural Sciences, Department of Physical Chemistry, Pirogova Street 2, Novosibirsk 630090, Russia

Supporting Information

ABSTRACT: A combination of experimental (quasi-elastic neutron scattering and ²H NMR) and computational (molecular dynamics) tools was used to uncover the molecular mobility of benzene trapped inside the flexible channel-type MIL-53 (Cr³⁺) MOF. This material was shown to undergo a contraction of the structure upon benzene adsorption with the formation of a narrow pore phase with a smaller aperture. This confinement was found to strongly influence the dynamics of the guest: benzene diffuses in a region centered in the middle of the pore by a 1D-jump translational mechanism along the tunnel ruled by the presence of the μ_2 -OH groups present at the MOF pore wall. This translational diffusion is combined with a fast uniaxial rotational motion around the C₆-axis. Any other rotational motion that involves the tumbling of the phenyl rings about the channel axis is much less probable due to a high activation energy barrier (49 kJ mol⁻¹). In this way benzene can be pictured as a rotating disc that diffuses rapidly through the central part of the channel by short jumps between neighboring low energy basins located in the vicinity of the μ_2 -OH groups of the MIL-53 channels.



1. INTRODUCTION

The porous metal–organic frameworks (MOFs) have attracted great attention during the past two decades for potential applications in a wide range of domains including energy, environment and health.^{1,2} In particular, some of these materials have been shown to be promising for the adsorption/separation of aromatics such as benzene and xylene isomers. This holds true for the microporous solids MIL-53(M³⁺ = Al³⁺, Cr³⁺, Fe³⁺) (MIL stands for Materials of the Institut Lavoisier)³ and its isostructural V⁴⁺-analogue MIL-47(V⁴⁺).^{4–12} These MOFs are built-up from infinite chains of corner-sharing M³⁺O₄(OH)₂ or V⁴⁺O₆ octahedra, interconnected by terephthalate ligands to create a 3D framework containing 1D diamond-shaped channels with pores of free diameter close to 8.5 Å. The adsorption properties of these latter solids with respect to a series of aromatics have been intensively explored experimentally and computationally with

the determination of adsorption isotherms and/or breakthrough curves.^{4–7} In contrast, only two studies were devoted to gain insight into the kinetics of the benzene and the xylenes molecules confined into the pores of MIL-47(V⁴⁺) with the evidence of an unusual diffusion mechanism corresponding to corkscrew motions along the channel.^{13,14} The dynamics of these aromatics is expected to be more complex in the MIL-53 series as these solids (i) contain hydroxyl functions present at the M³⁺-O-M³⁺ links (μ_2 -OH groups) which might act as strong attractive sites for the aromatics and/or as a steric barrier that hinders their mobility and (ii) undergo a structural contraction (also called as structural flexibility, or “breathing”) upon adsorption which leads to a narrower section available for the

Received: February 12, 2015

Revised: March 25, 2015

molecules to reorientate.^{3,15} As far as we know, neither experimental nor simulated data are reported yet on the dynamics of aromatics in such a breathing MOF.

To address this, here quasi-elastic neutron scattering (QENS) and ^2H nuclear magnetic resonance (NMR) experiments were coupled with molecular dynamics (MD) simulations to gain a fundamental understanding of the diffusion of benzene in the Cr^{3+} -version of MIL-53. Such a joint experimental/computational approach has been successfully employed to probe the diffusion of diverse guests in a variety of MOFs.^{13,16–28} The combination of QENS and ^2H NMR experiments operating over different time and length scales with molecular simulations allows a detailed description of the translational and rotational motions of the confined benzene molecules at the microscopic level. The diffusion mechanism in this breathing MOF as revealed by powder X-ray diffraction is compared to that previously evidenced on the rigid isostructural MIL-47(V^{4+}) material.

2. METHODOLOGY

Quasi-Elastic Neutron Scattering Measurements. The neutron experiments were carried out at the Institut Laue Langevin, using the time-of-flight (TOF) spectrometer IN5. The incident neutron wavelength was taken as 8 Å (corresponding energy 1.28 meV). After scattering by the sample, neutrons are analyzed as a function of time and angle. The TOF of the scattered neutrons is related to the energy transfer ($\hbar\omega$) and the scattering angle to the wave-vector transfer (Q). Spectra from different detectors are grouped, excluding the Bragg peaks of MIL-53(Cr^{3+}). The average wave-vector transfers ranged from 0.13 to 0.92 Å^{−1}. The TOF spectra resulting from the groupings are transformed to an energy scale after subtracting the scattering of the activated MOF. The elastic energy resolution can be fitted by a Gaussian function, with a half-width at half-maximum (HWHM) of the order of 11 μeV, depending on Q .

Perdeuterated MIL-53(Cr^{3+}) was used for the QENS experiments, to decrease the scattering from the organic linkers and from the hydroxyl groups. This solid was synthesized and activated according to the published procedures using deuterated terephthalic acid- d_4 (Euristotop, France) and hydrogenated solvent.³ After activation, the hydrogen atoms of the hydroxyl groups in MIL-53(Cr^{3+}) were exchanged for deuterium by stirring in deuterated water overnight. The MOF was activated at 473 K under vacuum and was then exposed to a volumetrically determined amount of liquid benzene, corresponding to 1 molecule/u.c. A second sample corresponded to the degassed MIL-53(Cr^{3+}), with a weight identical to the first sample. The two samples were transferred inside a glovebox into cylindrical aluminum containers of annular geometry. The containers were placed in a cryofurnace and the measurements were performed at four temperatures (300, 350, 400, and 450 K) to derive the activation energy for diffusion.

Nuclear Magnetic Resonance Measurements. ^2H NMR experiments were performed at 61.432 MHz on a Bruker Avance-400 spectrometer, using a high power probe with 5 mm horizontal solenoid coil. Metallic centers in the MIL-53(Cr^{3+}) structure are paramagnetic (Cr^{3+} , $S = 3/2$) which may influence the ^2H NMR spectrum by large frequency shifts and fast relaxation of the nuclear spin.²⁹ To compensate these effects and correctly refocus the ^2H NMR spectrum an Exorcycle quadrupole-echo sequence was used,³⁰ ($90_x - \tau_1 - 90_y - \tau_2 - \text{Acq} -$

t), where $\tau_1 = 20 \mu\text{s}$, $\tau_2 = 22 \mu\text{s}$, and t is a repetition time for the sequence during the accumulation of the NMR signal. The duration of the 90° pulses was 1.8–2.2 μs. To capture all dynamical features of the system, the measurements were performed over a broad temperature range, from 123 to 453 K. Perdeuterated benzene with 99.6% ^2H isotopic enrichment was purchased from SIGMA Aldrich, Inc. and used without further purification.

0.4 g of deuterated MIL-53(Cr^{3+}) was loaded in a 5 mm (o.d.) glass tube, connected to a vacuum system. The sample was heated at 473 K for 12 h in air and for 24 h under a vacuum of 10^{-5} Torr. After cooling back to room temperature, the solid was loaded with 1 benzene molecule per unit cell and sealed off. The adsorption was performed from the gas phase with the MOF powder kept at the temperature of liquid nitrogen. The sealed sample was then equilibrated at 373 K for 10 h.

X-ray Diffraction Measurements. The MIL-53(Cr^{3+}) sample was introduced in a glass capillary (diameter 0.5 mm) and heated under primary vacuum at 473 K for 8 h. A dose of benzene was loaded in the capillary in order to reach a low P/P^0 value of 0.004 at 303 K and the capillary was then flame-sealed. The powder X-ray diffraction (PXRD) patterns were then collected at room temperature on a PANalytical X'PERT II diffractometer using a monochromatic Cu- $K\alpha$ source ($\lambda = 1.5418 \text{ Å}$) with operating voltage of 40 kV and a beam current of 40 mA. The patterns were collected for 2θ from 2° to 75° . The unit-cell parameters were subsequently determined by indexing the PXRD pattern, using DICVOL6 followed by a Le Bail fit using FULLPROF.^{31–33}

Molecular Simulation. Crystal Structure Solution. The structure of MIL-53(Cr^{3+}) NP (Narrow Pore) in the presence of benzene was constructed starting from the crystallographic coordinates of the empty MIL-53(Cr^{3+}) LP (Large Pore) form³ and the unit cell parameters determined by the PXRD experiment. Following the strategy we successfully applied in the past to model the crystal structure of a series of MOFs,³⁴ this structure was energy-minimized at the force-field level. The energy function included a van der Waals contribution represented by a 12–6 Lennard-Jones expression whose parameters for all atoms of the framework were taken from the universal force field (UFF).³⁵ This crystal model was then loaded with 1 benzene molecule per unit cell and subsequently refined by density functional theory (DFT) calculations with the cell parameters fixed at the experimental XRPD values. These calculations were achieved using the PBE GGA density functional³⁶ and the double numerical basis containing polarization functions on hydrogen atoms (DNP)³⁷ as implemented in the Dmol³ code.³⁸

Molecular Dynamics Simulations. Molecular dynamics (MD) were performed at different temperatures ranging from 300 to 500 K using the DL_POLY program³⁹ in the NVT ensemble with the Berendsen thermostat.⁴⁰ The calculations considered a simulation box containing 32 ($2 \times 4 \times 4$) unit cells of the MIL-MIL-53(Cr^{3+}) NP form loaded with 16 benzene molecules to be consistent with the concentration explored experimentally. The initial configurations were generated by preliminary canonical Monte Carlo (CMC) simulations using the CADSS⁴¹ software with typically 10^7 Monte Carlo steps. Each MD calculation was then performed using 1×10^7 steps with a time step of 1 fs (i.e., 10 ns) preceded by 1 ns of equilibration. The self-diffusion coefficients, D_s were determined by fitting the mean-square displacements (MSD) plots assuming Einstein's relation.⁴⁰ To

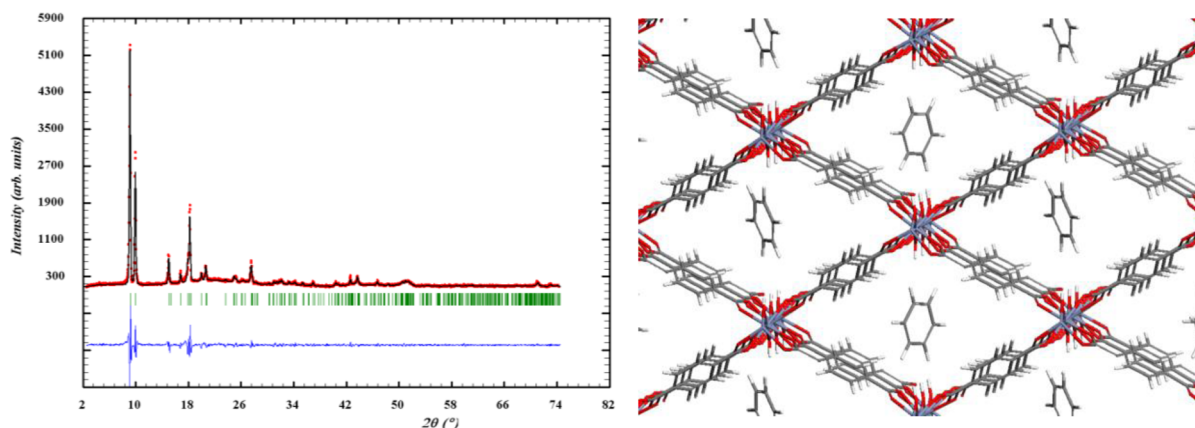


Figure 1. Structure-less pattern profile refinement of the experimental PXRD pattern collected for the benzene-loaded MIL-53(Cr³⁺) NP form (left). The plot reports the experimental (red) and calculated PXRD patterns (black), the difference curve (blue) and the position of the Bragg peaks (green) ($\lambda = 1.5406 \text{ \AA}$). DFT-predicted crystal structure for the benzene-loaded NP form (right).

improve the statistics of these calculations, the MSD were sampled for each temperature over 5 independent MD trajectories and the multiple time origins strategy was employed. The 2D free-energy maps were then obtained from the configurations stored during the MD runs using the histogram sampling method previously reported by Beerdse et al.⁴²

The interaction between the guest and the host was treated by a van der Waals term (12–6 Lennard-Jones expression) and a Coulombic contribution. While the benzene molecule was represented by the explicit charged model reported by Siepmann et al.,⁴³ the model for MIL-53(Cr³⁺) NP was taken from our previous studies⁴⁴ with the LJ parameters for each atom of the framework were considered from the generic universal force field (UFF)³⁵ and the partial charges extracted from a Mulliken partitioning scheme.⁴⁵ During the MD runs, the electrostatic interactions were calculated using the Ewald summation method and a cutoff of 12 Å was used for the short-range interactions.

3. RESULTS AND DISCUSSION

The adsorption of benzene in MIL-53(Cr³⁺) leads to significant changes of the neutron diffraction pattern with the appearance of new Bragg peaks which occurs concomitantly with an intensity decrease of those present initially (Figure S1). This observation is consistent with what has been already evidenced for this material upon the adsorption of a series of guest molecules. The presence of a heterogeneous distribution of crystallites leads to a phase mixture containing a large pore (LP) form with the structure that does not adsorb benzene and a more contracted structure when the guest molecules are present into its pore.^{15,34,44,46–51} The indexation of this contracted form was performed from the PXRD pattern collected on the benzene-loaded sample (see Figure S2) and compared to the data obtained from a LP form free of benzene (Figure S3). This confirmed the existence of a narrow pore (NP) monoclinic form (space group C2/c: $a = 19.146(2) \text{ \AA}$, $b = 11.525(1) \text{ \AA}$, $c = 6.840(1) \text{ \AA}$, $\beta = 112.159(7)^\circ$, $V = 1397.9(2) \text{ \AA}^3$) corresponding to a unit cell contraction of 6% (Figures 1 and S3). The crystal model of this NP form was built computationally by following the strategy described above (see Figure 1).

The diffusion of benzene in the NP form of MIL-53(Cr³⁺) is accessible on the time scale of the neutron experiment, in the

temperature range 300–450 K. The large influence of temperature on the spectral profile is apparent from Figure 2. The small value of the wave-vector transfer in that figure, $Q = 0.36 \text{ \AA}^{-1}$, ensures that the increase of the broadening of the elastic peak is due to fast long-range diffusion, the contribution from rotation at this Q value being small.⁵²

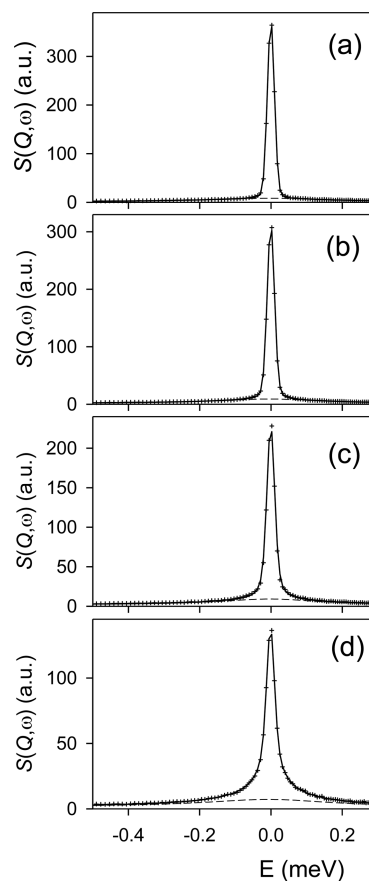


Figure 2. Comparison between experimental (crosses) and fitted (solid lines) QENS spectra obtained for benzene in MIL-53(Cr³⁺) at different temperatures: (a) 300, (b) 350, (c) 400, and (d) 450 K. The dashed lines indicate the contribution from rotation ($Q = 0.36 \text{ \AA}^{-1}$).

The Q dependence of the line shape at a given temperature is shown in Figure 3. At small Q , the contribution from rotation is negligible, this contribution increasing progressively with Q .

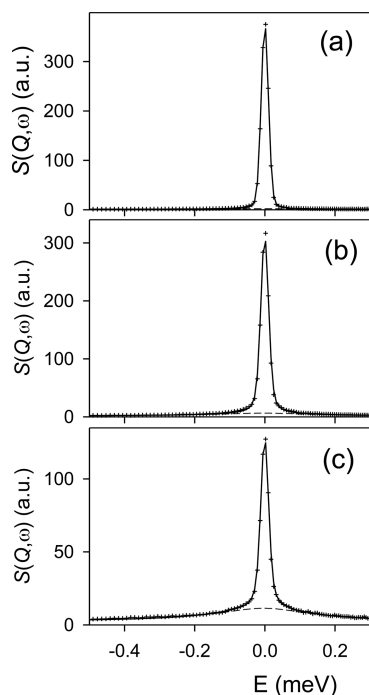


Figure 3. Comparison between experimental (crosses) and fitted (solid lines) QENS spectra obtained for benzene in MIL-53(Cr³⁺) at 400 K, for different Q values: (a) 0.13, (b) 0.26, (c) 0.5 Å^{−1}. The dashed lines indicate the contribution from rotation.

The measured intensities can be interpreted by analyzing self-motions of the hydrogen atoms, because of the large incoherent cross section of hydrogen. The spectra were fitted with a one-dimensional translational scattering function convoluted with a uniaxial rotational scattering function about the C_6 axis, and with the instrumental resolution. The line shape clearly corresponds to a 1D normal diffusion model,⁵³ where the molecules can pass each other in the MIL-53(Cr³⁺) tunnels. Single-file diffusion cannot account for the line shape as it yields a narrow peak with very large wings.⁵³ For the uniaxial rotation of benzene, the widths of the Lorentzian functions are related to the mean time τ between successive jumps,⁵⁴ which is on the picosecond time scale. The excellent agreement between experimental and calculated QENS spectra allows the derivation of the broadening due to translation with a good accuracy. The HWHMs obtained at four different temperatures are plotted in Figure 4 as a function of Q^2 .

At low temperatures, 300–400 K, the experimental points deviate from straight lines, and the trend is characteristic of jump diffusion with a distribution of jump lengths. At these temperatures, the Singwi–Sjölander jump diffusion model⁵⁵ allowed the simultaneous fitting of all spectra. A careful inspection of Figure 4b shows that the last two points ($Q^2 = 0.21$ and 0.26 Å^{−2}) tend to fall below the line, which could be captured by the Jobic model.⁵⁶ However, this will not affect the determination of the self-diffusion coefficients, which relies on the small Q range (corresponding to long distances).

At 450 K, the HWHM is proportional to Q^2 , as expected for continuous or Fickian diffusion.⁵² This regime was not reached

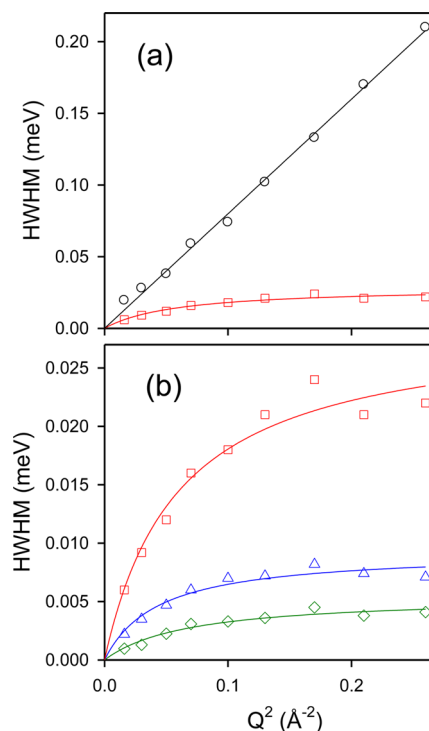


Figure 4. Broadenings of the elastic peak as a function of Q^2 due to the translation of benzene in MIL-53(Cr³⁺) at various temperatures: (\diamond) 300, (\triangle) 350, (\square) 400, and (\circ) 450 K. A common abscissa and two ordinate scales are used for parts a and b. The symbols correspond to individual fits of the spectra and the solid lines to simultaneous fits with a jump diffusion model.

for benzene in MIL-47(V⁴⁺), because of the lower temperature, 370 K.¹³

Analysis of the MD runs allowed us to get further insight into the microscopic diffusion mechanism in play. The 2D free energy maps for benzene were calculated at 300 K through planes perpendicular (XY) and parallel (YZ) to the channel of MIL-53(Cr³⁺) using the histogram sampling method (Figure 5). They show that the lower-energy regions are situated at the center of the pore. The minimum energy pathway, drawn by following the lower energy parts of Figure 5, reveals that the dynamics of benzene is mainly oriented along the direction of the tunnel with a sequence of jumps between regions in the vicinity of the μ_2 -OH groups. Inspection of the MD trajectories confirmed this diffusion profile as well as the absence of single-file diffusion, which both support the conclusions issued from the analysis of the QENS spectra. This behavior differs from the corkscrew type diffusion mechanism we previously evidenced in MIL-47(V⁴⁺). This is due to the combination of the smaller pore dimension of the NP version of MIL-53(Cr³⁺) and to the presence of μ_2 -OH groups which both rule the diffusion mechanism.

Figure 6 shows that the centers of mass of benzene are concentrated in a narrow corridor section localized very close to the center of the channel and that the molecules are preferentially oriented with their C_6 -axis nearly perpendicular to the tunnel (axis Z) associated with only a small amplitude of reorientation with respect to the channel plane (less than 20°). This holds for the whole temperature range explored. Such a distribution of molecules within the pores is consistent with the DFT optimized arrangement reported in Figure 1. The molecule behaves like a rotating disc with a translational

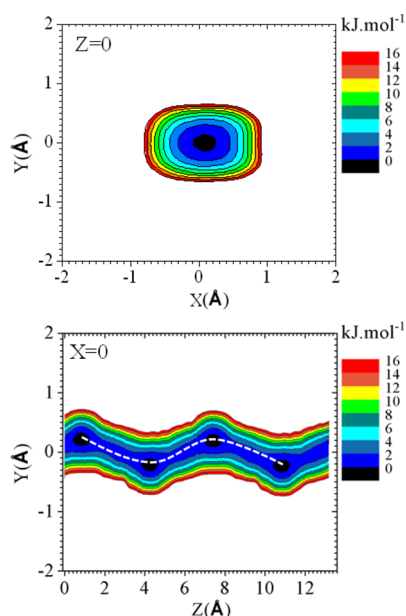


Figure 5. 2D slice of the free energy maps calculated at 300 K for benzene in the NP form of MIL-53(Cr³⁺) through the channel plane (XY, left) and along the channel direction (YZ, right). The dashed lines are guides to the eyes.

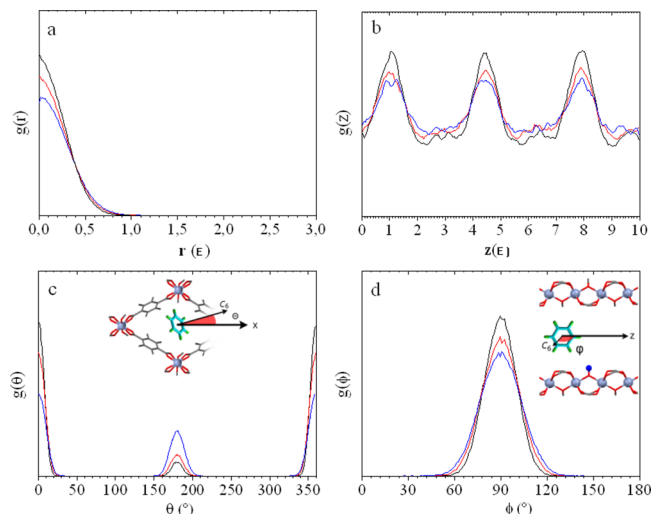


Figure 6. MD calculated distributions of the centers of mass of benzene in the NP form of MIL-53(Cr³⁺) radially from the center (a) and along the channel (b) with orientations of the C₆-axis in the channel plane (c) and along the tunnel (d). These data are reported at 300 (black), 400 (red), and 500 K (blue). φ and Θ correspond to the angle formed between the C₆-axis of benzene and the channel axis and channel plane, respectively.

motion along the channel axis combined with only reorientation around its C₆-axis.

The orientationally averaged QENS and MD self-diffusivities ($D_s = D_{1D}/3$) which are reported in Figure 7 agree within a factor of 2, while the activation energies calculated from the Arrhenius plots (17.0 kJ/mol vs 8.0 kJ/mol) deviate. These D_s are slightly lower than the experimental values we previously reported in MIL-47(V⁴⁺) (from 1.2 to 2.2×10^{-9} m²/s in the temperature range 300–370 K).¹³

In order to probe more precisely the rotational mobility of benzene inside the MIL-53(Cr³⁺) channels, we followed the ²H

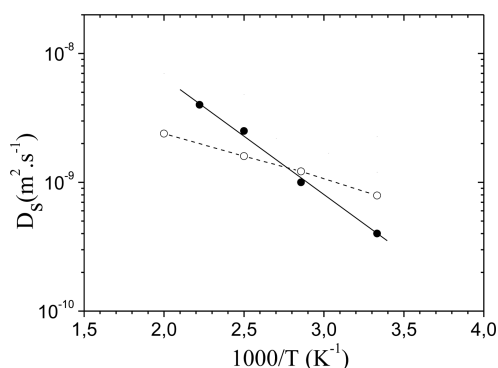


Figure 7. Self-diffusion coefficients for benzene in MIL-53(Cr): QENS (full symbols) and MD (empty symbols).

NMR spectra line shape evolution of the deuterated compound over a broad temperature region. The results are presented in Figure 8.

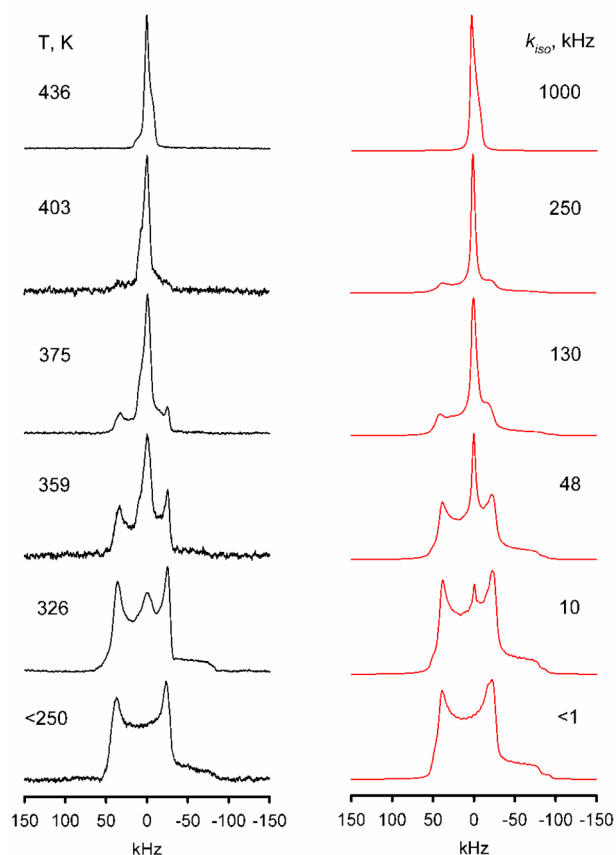


Figure 8. Benzene-*d*₆ ²H NMR spectra line shape temperature evolution in MIL-53(Cr): experimental results (left); simulated results (right).

The experimental line shape evolves from a broad and purely anisotropic pattern monitored between 100 and 250 K, up to a narrow one, close to liquid-like shape above 430 K. The anisotropic line shape monitored below 250 K is given by a distorted Pake-powder pattern with an effective value of the interaction constant $Q_{\text{eff}} = Q_0/2 - 85$ kHz. The observed Q_{eff} value is characteristic of a fast uniaxial rotation of benzene about the C₆ symmetry axis.^{13,57,58}

Such a dynamical behavior is typical for benzene in bulk state,^{57,58} adsorbed in mesoporous silica gels,⁵⁸ microporous zeolites^{59–65} and MOFs MIL-47(V⁴⁺)¹³ and MOF-5.⁶⁶ In almost all reported cases, the C₆ rotation of benzene is characterized by the lowest activation barrier and it represents the fastest intramolecular dynamical mode.

At the same time, the spectrum line shape notably differs from the axial symmetry expected for a fast uniaxial rotation around C₆.¹³ The observed distortions in ²H NMR spectra line shapes are a consequence of strong electron–nuclear dipolar interaction of deuterium spin with the Cr³⁺ paramagnetic centers of the MIL-53(Cr³⁺) framework. Therefore, in order to quantify the benzene mobility, one has to take into account this paramagnetic interaction. The general formalism needed to compute the paramagnetic distortions in ²H NMR spectra is well-known^{30,67} and it can be applied in the case of defined geometries, i.e., when for each paramagnetic site the distance and orientation of its *g*-tensor and its own position relative to the chosen deuterium site can be calculated from crystallographic data.⁶⁷ These parameters can be used to compute the distortion frequencies to be further introduced in a standard manner into the fitting routine (see Figure S4).

The strength of interaction with paramagnetic ions is proportional to their total electron spin and it rapidly decreases with distances ($\sim 1/r^3$), thus only the closest to paramagnetic ion centers should be considered. For instance, such an approach allowed us to correctly reproduce the ²H NMR spectrum of deuterated linkers in MIL-53(Cr³⁺) by taking into account only 8 closest Cr³⁺ ions.⁶⁶ In the present case, however, the position of benzene inside the channels also needs to be defined. The QENS data shows that benzene rapidly diffuses along the channel (i.e., the Z axis) with a fast rotation about the C₆ axis. The ²H NMR spectra line shape is not changed at 100 K–250 K, which suggests that apart from the uniaxial C₆ rotation no other rotational motion faster than 10³ Hz is present. Thus, below 250 K, benzene can be indeed seen as a rotating disc diffusing in the middle of the channel, as also evidenced at 300 K by MD simulations. Since these two motions are clearly fast on the ²H NMR time scale, one can assume that the influence from different paramagnetic centers is averaged. This can be used to define the geometrical parameters for the model of benzene interaction with paramagnetic centers inside the MOF channel.

The Cr³⁺ ions occupy the corners of the MIL-53 channel cross-section and form a chain along its Z axis. Considering this symmetry, one can assume that each chain of ions can be represented by one paramagnetic center with an effective interaction tensor (see Figure 1). The effective paramagnetic interaction constant can be regarded as the effective value of the isotropic *g*-tensor, but physically it is mainly related to the averaged distance between the deuterium and the paramagnetic site and the orientation change. As a first step of spectra simulation, we need to tune the effective interaction constant. The line shape is not changed at 100–250 K, and we can assume that it is influenced only by the C₆ axis rotation with the rotation rate found in the fast exchange limit. The polar (rotation) angle between the C₆ axis and the C–D bond direction for the geometry of benzene is $\theta_{C_6} = 90^\circ$. Figure 8 shows that such an approach allows a perfect fit of the experimental line shape. Models that assumed the position of the benzene ring closer to one of the walls showed bad agreement with the experimental line shapes.

Further, an additional motion should be introduced to reproduce the temperature evolution of the line shape above 250 K. In addition to the C₆ rotation, benzene can exhibit anisotropic reorientations around its C₂ axes. Isotropic reorientation could represent another possibility. The real isotropic reorientation is a continuous rotational diffusion, while the pseudoisotropic reorientation is a motion represented by discrete jumps with sufficiently high symmetry (i.e., tetrahedral or octahedral).¹³ After trying different models, it was found that only the pseudoisotropic reorientation model allowed a nice fit of the experimental data. The temperature dependence of the reorientation jump rate follows an Arrhenius law (see Figure 9) with an associated activation barrier of 49 kJ mol^{−1} and a pre-exponential factor $k_0 = 6.1 \times 10^{11}$ s^{−1}.

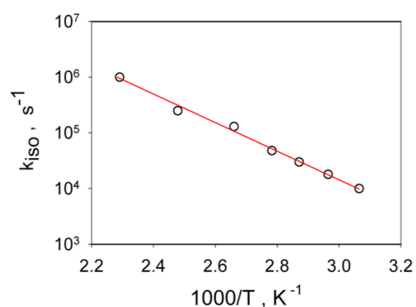


Figure 9. Arrhenius plot of the pseudoisotropic jump reorientation rate constant.

Such a high pre-exponential factor indicates that this motion is of local nature, which is in contrast with the situation observed in MIL-47(V⁴⁺).¹³ However, due to the high activation barrier its resulting rate is rather low, i.e. at moderate temperatures ($T < 400$ K) these out-of-plane reorientations are strongly hindered. For the same reason this dynamics is not captured by our MD simulations. This experimental result fully supports the dynamical behavior pictured by QENS and MD and emphasizes the high degree of confinement for benzene in the MIL-53 (Cr³⁺) NP structure.

4. CONCLUSION

Three dynamical techniques (QENS, ²H NMR and MD) have been intertwined to cover broad time and length scales to reveal the diffusion mechanism of benzene confined into the pore of the flexible MIL-53 (Cr³⁺). It was established that the guest adsorption induces a contraction of the structure toward a narrow pore form which restricts the diffusion of the guest in a region centered at the middle of the pore. The benzene diffuses via (i) a 1D-jump translational mechanism along the tunnel with its C₆-axis perpendicular to the channel axis, ruled by the presence of the μ_2 -OH groups at the MOF pore wall, combined with (ii) a fast uniaxial rotational motion around the C₆-axis. Any other rotational motion that involves the tumbling of the phenyl rings about the channel axis is much less probable due to a high activation energy barrier (49 kJ mol^{−1}) more than three times higher than in MIL-47(V⁴⁺). Indeed benzene can be seen as a rotating disc that diffuses rapidly through the central part of the channel by short jumps between neighboring low energy basins located in the vicinity of the μ_2 -OH groups of the MIL-53(Cr³⁺) channels. This dynamical behavior significantly deviates with the corkscrew motion previously elucidated in the nonbreathing MIL-47(V⁴⁺) and clearly emphasizes that not only the contraction of the structure but also the presence of the μ_2 -

OH groups govern the host/guest interactions and thus the diffusion mechanism in play.

■ ASSOCIATED CONTENT

● Supporting Information

Figures S1–S4, showing neutron diffraction patterns, structure-independent refinements of the unit-cell of the diffraction pattern, X-ray diffraction patterns, and a diagram of the paramagnetic Cr³⁺ site. This material is available free of charge via the Internet at <http://pubs.acs.org>.

■ AUTHOR INFORMATION

Corresponding Authors

*(H.J.) E-mail: herve.jobic@ircelyon.univ-lyon1.fr. Telephone: +33 4 72 44 53 01.

*(G.M.) E-mail: guillaume.maurin@univ-montp2.fr. Telephone: +33 4 67 14 33 07.

Author Contributions

The manuscript was written through contributions of all authors.

Notes

The authors declare no competing financial interest.

■ ACKNOWLEDGMENTS

The authors thank the Institut Lavoisier UMR CNRS 8180–Université de Versailles St Quentin en Yvelines (V. Guillermin, T. Devic, C. Serre) for providing the deuterated MIL-53(Cr³⁺) sample and the Institut Laue–Langevin for allocating neutron beam time on IN5. D.I.K. and A.G.S. thank Russian Foundation for Basic Research (Grant No. 14-03-91333) for support. G.M. thanks the Institut universitaire de France for its support.

■ REFERENCES

- (1) Zhou, H.-C.; Kitagawa, S. Themed Collection Metal–Organic Frameworks (MOFs). *Chem. Soc. Rev.* **2014**, *43*, 5415–5418.
- (2) Zhou, H.-C.; Long, J. R.; Yaghi, O. M. Introduction to Metal–Organic Frameworks. *Chem. Rev.* **2012**, *112*, 673–674.
- (3) Serre, C.; Millange, F.; Thouvenot, C.; Nogues, M.; Marsolier, G.; Louer, D.; Férey, G. Very Large Breathing Effect in the First Nanoporous Chromium(III)-Based Solids: MIL-53 or CrIII(OH), {O₂C–C₆H₄–CO₂}, {HO₂C–C₆H₄–CO₂H}₂·H₂O₂. *J. Am. Chem. Soc.* **2002**, *124*, 13519–13526.
- (4) Finsy, V.; Kirschhock, C. E. A.; Vedts, G.; Maes, M.; Alaerts, L.; De Vos, D. E.; Baron, G. V.; Denayer, J. F. M. Framework Breathing in the Vapour-Phase Adsorption and Separation of Xylene Isomers with the Metal–Organic Framework MIL-53. *Chem.—Eur. J.* **2009**, *15*, 7724–7731.
- (5) Moreira, M. A.; Santos, J. C.; Ferreira, A. F. P.; Loureiro, J. M.; Rodrigues, A. E. Influence of the Eluent in the MIL-53(Al) Selectivity for Xylene Isomers Separation. *Ind. Eng. Chem. Res.* **2011**, *50*, 7688–7695.
- (6) Moreira, M. A.; Santos, J. C.; Ferreira, A. F. P.; Muller, U.; Trukhan, N.; Loureiro, J. M.; Rodrigues, A. E. Selective Liquid Phase Separation of ortho-Xylene with the Microporous MIL-53(Al). *Sep. Sci. Technol.* **2011**, *46*, 1995–2003.
- (7) El Osta, R.; Carlin-Sinclair, A.; Guillou, N.; Walton, R. I.; Vermoortele, F.; Maes, M.; de Vos, D.; Millange, F. Liquid-Phase Adsorption and Separation of Xylene Isomers by the Flexible Porous Metal–Organic Framework MIL-53(Fe). *Chem. Mater.* **2012**, *24*, 2781–2791.
- (8) Alaerts, L.; Kirschhock, C. E. A.; Maes, M.; van der Veen, M. A.; Finsy, V.; Depla, A.; Martens, J. A.; Baron, G. V.; Jacobs, P. A.; Denayer, J. E. M.; De Vos, D. E. Selective Adsorption and Separation of Xylene Isomers and Ethylbenzene with the Microporous Vanadium(IV) Terephthalate MIL-47. *Angew. Chem., Int. Ed.* **2007**, *46*, 4293–4297.
- (9) Finsy, V.; Verelst, H.; Alaerts, L.; De Vos, D.; Jacobs, P. A.; Baron, G. V.; Denayer, J. F. M. Pore-Filling-Dependent Selectivity Effects in the Vapor-Phase Separation of Xylene Isomers on the Metal–Organic Framework MIL-47. *J. Am. Chem. Soc.* **2008**, *130*, 7110–7118.
- (10) Maes, M.; Vermoortele, F.; Boulhout, M.; Boudewijns, T.; Kirschhock, C.; Ameloot, R.; Beurroies, I.; Denoyel, R.; De Vos, D. E. Enthalpic Effects in the Adsorption of Alkylaromatics in the Metal–Organic Frameworks MIL-47 and MIL-53. *Microporous Mesoporous Mater.* **2012**, *157*, 82–88.
- (11) Ghysels, A.; Vandichel, M.; Verstraeten, T.; van der Veen, M. A.; De Vos, D. E.; Waroquier, M.; Van Speybroeck, V. Host-Guest and Guest-Guest Interactions between Xylene Isomers Confined in the MIL-47(V) Pore System. *Theor. Chem. Acc.* **2012**, *131*, 1234–1246.
- (12) Barthelet, K.; Marrot, J.; Riou, D.; Férey, G. A Breathing Hybrid Organic-Inorganic Solid with Very Large Pores and High Magnetic Characteristics. *Angew. Chem., Int. Ed.* **2002**, *41*, 281–284.
- (13) Kolokolov, D. I.; Jobic, H.; Stepanov, A. G.; Ollivier, J.; Rives, S.; Maurin, G.; Devic, T.; Serre, C.; Férey, G. Experimental and Simulation Evidence of a Corkscrew Motion for Benzene in the Metal–Organic Framework MIL-47. *J. Phys. Chem. C* **2012**, *116*, 15093–15098.
- (14) Rives, S.; Jobic, H.; Kolokolov, D. I.; Gabrienko, A. A.; Stepanov, A. G.; Ke, Y.; Frick, B.; Devic, T.; Férey, G.; Maurin, G. Diffusion of Xylene Isomers in the MIL-47 (V) MOF Material: a Synergic Combination of Computational and Experimental Tools. *J. Phys. Chem. C* **2013**, *117*, 6293–6302.
- (15) Férey, G.; Serre, C.; Devic, T.; Maurin, G.; Jobic, H.; Llewellyn, P. L.; De Weireld, G.; Vimont, A.; Daturi, M.; Chang, J. S. Why Hybrid Porous Solids Capture Greenhouse Gases? *Chem. Soc. Rev.* **2011**, *40*, 550–562.
- (16) Salles, F.; Jobic, H.; Maurin, G.; Koza, M. M.; Llewellyn, P. L.; Devic, T.; Serre, C.; Férey, G. Experimental Evidence Supported by Simulations of a Very High H₂ Diffusion in Metal Organic Framework Materials. *Phys. Rev. Lett.* **2008**, *100*, 245901.1–245901.4.
- (17) Salles, F.; Kolokolov, D. I.; Jobic, H.; Maurin, G.; Llewellyn, P. L.; Devic, T.; Serre, C.; Férey, G. Adsorption and Diffusion of H-2 in the MOF Type Systems MIL-47(V) and MIL-53(Cr): A Combination of Microcalorimetry and QENS Experiments with Molecular Simulations. *J. Phys. Chem. C* **2009**, *113*, 7802–7812.
- (18) Salles, F.; Jobic, H.; Devic, T.; Llewellyn, P. L.; Serre, C.; Férey, G.; Maurin, G. Self and Transport Diffusivity of CO₂ in the Metal–Organic Framework MIL-47(V) Explored by Quasi-elastic Neutron Scattering Experiments and Molecular Dynamics Simulations. *ACS Nano* **2010**, *4*, 143–152.
- (19) Rosenbach, N.; Jobic, H.; Ghoufi, A.; Salles, F.; Maurin, G.; Bourrelly, S.; Llewellyn, P. L.; Devic, T.; Serre, C.; Férey, G. Quasi-Elastic Neutron Scattering and Molecular Dynamics Study of Methane Diffusion in Metal–Organic Frameworks MIL-47(V) and MIL-53(Cr). *Angew. Chem., Int. Ed.* **2008**, *47*, 6611–6615.
- (20) Jobic, H.; Rosenbach, N.; Ghoufi, A.; Kolokolov, D. I.; Yot, P. G.; Devic, T.; Serre, C.; Férey, G.; Maurin, G. Unusual Chain-Length Dependence of the Diffusion of n-Alkanes in the Metal–Organic Framework MIL-47(V): The Blowgun Effect. *Chem.—Eur. J.* **2010**, *16*, 10337–10341.
- (21) Rives, S.; Jobic, H.; Ragon, F.; Devic, T.; Serre, C.; Férey, G.; Ollivier, J.; Maurin, G. Diffusion of Long Chain n-Alkanes in the Metal–Organic Framework MIL-47(V): A Combination of Neutron Scattering Experiments and Molecular Dynamics Simulations. *Microporous Mesoporous Mater.* **2012**, *164*, 259–265.
- (22) Salles, F.; Jobic, H.; Ghoufi, A.; Llewellyn, P. L.; Serre, C.; Bourrelly, S.; Férey, G.; Maurin, G. Transport Diffusivity of CO₂ in the Highly Flexible Metal–Organic Framework MIL-53(Cr). *Angew. Chem., Int. Ed.* **2009**, *48*, 8335–8339.
- (23) Salles, F.; Bourrelly, S.; Jobic, H.; Devic, T.; Guillermin, V.; Llewellyn, P.; Serre, C.; Férey, G.; Maurin, G. Molecular Insight into the Adsorption and Diffusion of Water in the Versatile Hydrophilic/

- Hydrophobic Flexible MIL-53(Cr) MOF. *J. Phys. Chem. C* **2011**, *115*, 10764–10776.
- (24) Yang, Q. Y.; Wiersum, A. D.; Jobic, H.; Guillermin, V.; Serre, C.; Llewellyn, P. L.; Maurin, G. Understanding the Thermodynamic and Kinetic Behavior of the CO₂/CH₄ Gas Mixture within the Porous Zirconium Terephthalate UiO-66(Zr): A Joint Experimental and Modeling Approach. *J. Phys. Chem. C* **2011**, *115*, 13768–13774.
- (25) Yang, Q. Y.; Jobic, H.; Salles, F.; Kolokolov, D.; Guillermin, V.; Serre, C.; Maurin, G. Probing the Dynamics of CO(2) and CH(4) within the Porous Zirconium Terephthalate UiO-66(Zr): A Synergic Combination of Neutron Scattering Measurements and Molecular Simulations. *Chem.—Eur. J.* **2011**, *17*, 8882–8889.
- (26) Yang, Q.; Vaesen, S.; Ragon, F.; Wiersum, A. D.; Wu, D.; Lago, A.; Devic, T.; Martineau, C.; Taulelle, F.; Llewellyn, P. L.; Jobic, H.; Zhong, C.; Serre, C.; De Weireld, G.; Maurin, G. A Water Stable Metal–Organic Framework with Optimal Features for CO₂ Capture. *Angew. Chem., Int. Ed.* **2013**, *52*, 10316–10320.
- (27) Ramsahye, N. A.; Gao, J.; Jobic, H.; Llewellyn, P. L.; Yang, Q.; Wiersum, A. D.; Koza, M. M.; Guillermin, V.; Serre, C.; Zhong, C. L.; Maurin, G. Adsorption and Diffusion of Light Hydrocarbons in UiO-66(Zr): A Combination of Experimental and Modeling Tools. *J. Phys. Chem. C* **2014**, *118*, 27470–27482.
- (28) Rosenbach, N.; Jobic, H.; Ghoufi, A.; Devic, T.; Koza, M. M.; Ramsahye, N.; Mota, C. J.; Serre, C.; Maurin, G. Diffusion of Light Hydrocarbons in the Flexible MIL-53(Cr) Metal–Organic Framework: A Combination of Quasi-Elastic Neutron Scattering Experiments and Molecular Dynamics Simulations. *J. Phys. Chem. C* **2014**, *118*, 14471–14477.
- (29) Mizuno, M.; Itakura, N.; Endo, K. Effects of Strong Paramagnetic Interactions on Solid-State Deuterium NMR Spectra. *Chem. Phys. Lett.* **2005**, *416*, 358–363.
- (30) Antonijevic, S.; Wimperis, S. Refocussing of Chemical and Paramagnetic Shift Anisotropies in ²H NMR Using the Quadrupolar-Echo Experiment. *J. Magn. Reson.* **2003**, *164*, 343–350.
- (31) Boulitf, A.; Louer, D. Indexing of powder diffraction patterns for low-symmetry lattices by the successive dichotomy method. *J. Appl. Crystallogr.* **1991**, *24*, 987–993.
- (32) Rodriguez-Carvajal, J. A program for Rietveld refinement and pattern matching analysis. *Collect. Abstr. Powder Diffraction Meet.* **1990**, 127–128.
- (33) Roisnel, T.; Rodriguez-Carvajal, J. WinPLOTR: A Windows Tool for Powder Diffraction Patterns Analysis. In *Proceedings of the Seventh European Powder Diffraction Conference*; Materials Science Forum: Barcelona, Spain, 2000; pp 118–123.
- (34) Llewellyn, P. L.; Maurin, G.; Devic, T.; Loera-Serna, S.; Rosenbach, N.; Serre, C.; Bourrelly, S.; Horcajada, P.; Filinchuk, Y.; Férey, G. Prediction of the Conditions for Breathing of Metal-Organic Framework Materials Using a Combination of X-ray Powder Diffraction, Microcalorimetry, and Molecular Simulation. *J. Am. Chem. Soc.* **2008**, *130*, 12808–12814.
- (35) Rappe, A. K.; Casewit, C. J.; Colwell, K. S.; Goddard, W. A.; Skiff, W. M. UFF, a Full Periodic-Table Force-Field for Molecular Mechanics and Molecular-Dynamics Simulations. *J. Am. Chem. Soc.* **1992**, *114*, 10024–10035.
- (36) Perdew, J. P.; Burke, K.; Ernzerhof, M. Generalized Gradient Approximation Made Simple. *Phys. Rev. Lett.* **1996**, *77*, 3865–3868.
- (37) Hehre, W. J.; Ditchfield, R.; Pople, J. A. Self-Consistent Molecular Orbital Methods. XII. Further Extensions of Gaussian-Type Basis Sets for Use in Molecular Orbital Studies of Organic Molecules. *J. Chem. Phys.* **1972**, *56*, 2257–2261.
- (38) Accelrys, Inc. Materials Studio, v. 5.0. San Diego 2009.
- (39) Smith, W.; Forester, T. R. DL_POLY_2.0: A general-Purpose Parallel Molecular Dynamics Simulation Package. *J. Mol. Graphics* **1996**, *14*, 136–141.
- (40) Frenkel, D.; Smit, B. *Understanding Molecular Simulation, Second Edition: From Algorithms to Applications*; Academic Press: New York, 2001.
- (41) Yang, Q.; Zhong, C. Molecular Simulation of Carbon Dioxide/methane/hydrogen Mixture Adsorption in Metal-Organic Frameworks. *J. Phys. Chem. B* **2006**, *110*, 17776–17783.
- (42) Beerdse, E.; Smit, B.; Dubbeldam, D. Molecular Simulation of Loading Dependent Slow Diffusion in Confined Systems. *Phys. Rev. Lett.* **2004**, *93*, 248301.
- (43) Rai, N.; Siepmann, J. I.; Schultz, N. E.; Ross, R. B. Pressure Dependence of the Hildebrand Solubility Parameter and the Internal Pressure: Monte Carlo Simulations for External Pressures up to 300 MPa. *J. Phys. Chem. C* **2007**, *111*, 15634–15641.
- (44) Salles, F.; Ghoufi, A.; Maurin, G.; Bell, R. G.; Mellot-Draznieks, C.; Férey, G. Molecular Dynamics Simulations of Breathing MOFs: Structural Transformations of MIL-53(Cr) upon Thermal Activation and CO₂ Adsorption. *Angew. Chem.-Int. Ed.* **2008**, *47*, 8487–8491.
- (45) Ramsahye, N. A.; Maurin, G.; Bourrelly, S.; Llewellyn, P.; Loiseau, T.; Férey, G. Charge Distribution in Metal-Organic Framework Materials: Transferability to a Preliminary Molecular Simulation Study of the CO₂ Adsorption in the MIL-53 (Al) System. *Phys. Chem. Chem. Phys.* **2007**, *9*, 1059–1063.
- (46) Rosenbach, N.; Ghoufi, A.; Deroche, I.; Llewellyn, P. L.; Devic, T.; Bourrelly, S.; Serre, C.; Férey, G.; Maurin, G. Adsorption of Light Hydrocarbons in the Flexible MIL-53(Cr) and Rigid MIL-47(V) Metal-Organic Frameworks: a Combination of Molecular Simulations and Microcalorimetry/Gravimetry Measurements. *Phys. Chem. Chem. Phys.* **2010**, *12*, 6428–6437.
- (47) Ghoufi, A.; Maurin, G. Hybrid Monte Carlo Simulations Combined with a Phase Mixture Model to Predict the Structural Transitions of a Porous Metal-Organic Framework Material upon Adsorption of Guest Molecules. *J. Phys. Chem. C* **2010**, *114*, 6496–6502.
- (48) Horcajada, P.; Gref, R.; Baati, T.; Allan, P. K.; Maurin, G.; Couvreur, P.; Férey, G.; Morris, R.; Serre, C. Metal-Organic Frameworks in Biomedicine. *Chem. Rev.* **2012**, *112*, 1232–1268.
- (49) Ghoufi, A.; Subercaze, A.; Ma, Q.; Yot, P. G.; Ke, Y.; Puente Orench, I.; Devic, T.; Guillermin, V.; Zhong, C.; Serre, C.; Férey, G.; Maurin, G. Comparative Guest, Thermal, and Mechanical Breathing of the Porous Metal Organic Framework MIL-53(Cr): A Computational Exploration Supported by Experiments. *J. Phys. Chem. C* **2012**, *116*, 13289–13295.
- (50) Bourrelly, S.; Moulin, B.; Rivera, A.; Maurin, G.; Devautour-Vinot, S.; Serre, C.; Devic, T.; Horcajada, P.; Vimont, A.; Clet, G.; Daturi, M.; Lavalley, J. C.; Loera-Serna, S.; Denoyel, R.; Llewellyn, P. L.; Férey, G. Explanation of the Adsorption of Polar Vapors in the Highly Flexible Metal Organic Framework MIL-53(Cr). *J. Am. Chem. Soc.* **2010**, *132*, 9488–9498.
- (51) Serre, C.; Bourrelly, S.; Vimont, A.; Ramsahye, N. A.; Maurin, G.; Llewellyn, P. L.; Daturi, M.; Filinchuk, Y.; Leynaud, O.; Barnes, P.; Férey, G. An Explanation for the Very Large Breathing Effect of a Metal-Organic Framework During CO₂ Adsorption. *Adv. Mater.* **2007**, *19*, 2246–2251.
- (52) Jobic, H.; Theodorou, D. N. Quasi-Elastic Neutron Scattering and Molecular Dynamics Simulation as Complementary Techniques for Studying Diffusion in Zeolites. *Microporous Mesoporous Mater.* **2007**, *102*, 21–50.
- (53) Jobic, H.; Hahn, K.; Karger, J.; Bee, M.; Tuel, A.; Noack, M.; Gurns, I.; Kearley, G. J. Unidirectional and Single-File Diffusion of Molecules in One-Dimensional Channel Systems. A Quasi-Elastic Neutron Scattering Study. *J. Phys. Chem. B* **1997**, *101*, 5834–5841.
- (54) Jobic, H.; Bée, M.; Renouprez, A. Quasi-Elastic Neutron Scattering of Benzene in Na-Mordenite. *Surf. Sci.* **1984**, *140*, 307–320.
- (55) Singwi, K. S.; Sjölander, A. Diffusive Motions in Water and Cold Neutron Scattering. *Phys. Rev.* **1960**, *119*, 863–871.
- (56) Gergidis, L. N.; Theodorou, D. N.; Jobic, H. Dynamics of n-Butane-Methane Mixtures in Silicalite, Using Quasielastic Neutron Scattering and Molecular Dynamics Simulations. *J. Phys. Chem. B* **2000**, *104*, 5541–5552.
- (57) Ok, J. H.; Vold, R. R.; Vold, R. L.; Etter, M. C. Deuterium NMR Measurements of Rotation and Libration of Benzene in a Solid-State Cyclamer. *J. Phys. Chem.* **1989**, *93*, 7618–7624.

- (58) Gedat, E.; Schreiber, A.; Albrecht, J.; Emmeler, T.; Shenderovich, I.; Findenegg, G. H.; Limbach, H.-H.; Buntkowsky, G. ^2H Solid-State NMR Study of Benzene- d_6 Confined in Mesoporous Silica SBA-15. *J. Phys. Chem. B* **2002**, *106*, 1977–1984.
- (59) Gedeon, A.; Favre, D. E.; Reichert, D.; MacNeil, J.; Chmelka, B. F. Distributions of Site-Hopping Geometries and Rates for Benzene Adsorbed on Ag-Y Zeolite. *J. Phys. Chem. A* **1999**, *103*, 6691–6703.
- (60) Docquir, F.; Norberg, V.; Su, B. L. Mobility of Benzene Molecules in NaEMT and KL Zeolitic Nanostructures Studied by ^2H NMR Spin-Lattice Relaxation Experiments. *Chem. Phys. Lett.* **2004**, *387*, 188–192.
- (61) Norberg, V.; Docquir, F.; Su, B. L. Behavior of Benzene Molecules in Large Pore Zeolite Structures as Studied by FTIR and ^2H NMR Techniques In *Porous Materials in Environmentally Friendly Processes*; Kiricsi, I., PalBorbely, G., Nagy, J., Karge, H., Eds.; ELSEVIER Science PUBL B V: Amsterdam, 1999; Vol. 125, pp 253–260.
- (62) Zibrowius, B.; Caro, J.; Pfeifer, H. Deuterium Nuclear Magnetic Resonance Studies of the Molecular Dynamics of Benzene in Zeolites. *J. Chem. Soc., Faraday Trans. 1* **1988**, *84*, 2347–2356.
- (63) Portsmouth, R. L.; Duerb, M. J.; Gladden, L. F. ^2H NMR Studies of Single-component Adsorption in Silicalite: A Comparative Study of Benzene and p-Xylene. *J. Chem. Soc. Faraday Trans.* **1995**, *91*, 559–567.
- (64) Geil, B.; Isfort, O.; Boddenberg, B.; Favre, D. E.; Chmelka, B. F.; Fujara, F. Reorientational and Translational Dynamics of Benzene in Zeolite NaY as Studied by One- and Two-Dimensional Exchange Spectroscopy and Static-Field-Gradient Nuclear Magnetic Resonance. *J. Chem. Phys.* **2002**, *116*, 2184–2193.
- (65) Eckman, R. R.; Vega, A. J. Deuterium Solid-state NMR Study of the Dynamics of Molecules Sorbed by Zeolites. *J. Phys. Chem.* **1986**, *90*, 4679–4683.
- (66) Gonzalez, J.; Devi, R. N.; Tunstall, D. P.; Cox, P. A.; Wright, P. A. Deuterium NMR Studies of Framework and Guest Mobility in the Metal-Organic Framework Compound MOF-5, $\text{Zn}_4\text{O}(\text{O}_2\text{CC}_6\text{H}_4\text{CO}_2)(3)$. *Microporous Mesoporous Mater.* **2005**, *84*, 97–104.
- (67) Kolokolov, D. I.; Jobic, H.; Stepanov, A. G.; Guillermin, V.; Devic, T.; Serre, C.; Férey, G. Dynamics of Benzene Rings in MIL-53(Cr) and MIL-47(V) Frameworks Studied by ^2H NMR Spectroscopy. *Angew. Chem., Int. Ed.* **2010**, *49*, 4791–4794.